Solar Energy Materials and Solar Cells 173 (2017) 37–42

Contents lists available at ScienceDirect

Solar Energy Materials and Solar Cells

journal homepage: www.elsevier.com/locate/solmat

Exceeding conversion efficiency of 26% by heterojunction interdigitated back contact solar cell with thin film Si technology

Kunta Yoshikawa*, Wataru Yoshida, Toru Irie, Hayato Kawasaki, Katsunori Konishi, Hirotaka Ishibashi, Tsuyoshi Asatani, Daisuke Adachi, Masanori Kanematsu, Hisashi Uzu, Kenji Yamamoto

KANEKA Corporation, 5-1-1 Torikai-Nishi, Settsu, Osaka 566-0072, Japan

ARTICLE INFO

Keywords:
Solar cell
Heterojunction
Back contact

ABSTRACT

We have developed heterojunction interdigitated back contact solar cell with conversion efficiency of 26.6% (designated area: 180 cm^2) independently confirmed by Fraunhofer Institute for Solar Energysystem Callab. Compared to our previous record efficiency (26.3%), the 0.3% absolute improvement can be regarded as ~10% reduction of remaining losses to the theoretical limit (~ 29%). We discuss the analyzed cell properties together with our recent progress to predict how far we can go in reducing the remaining losses in silicon photovoltaic.

1. Introduction

The conversion efficiency of crystalline silicon (Si) solar cell has been improving continuously after the invention of solar cell and have reached 25% (designated area: 4 cm^2) in 1999 [1]. Recently, high efficiency results exceeding 25% were reported by several groups using different device architectures. Heterojunction interdigitated back contact (HJ-IBC) cell with efficiency of 25.6% [2], interdigitated back contact (IBC) cell with efficiency of 25.2% [3], top/rear contacted heterojunction (HJ) with efficiency of 25.1% [4] and top/rear contacted cell using front homojunction emitter and rear thin oxide passivated contact (TOPCon) with efficiency of 25.7% [5,6] were reported respectively. We have reported 26.3% by HJ-IBC solar cell which was the first Si solar cell to exceed 26% conversion efficiency [7]. We have also estimated the practical limit efficiency to be 27.1% using cell characteristic of 26.3% and lifetime from the passivated sample [7]. Setting such practical limit helps to know where we are and to decide which item to focus on.

It can be said that these recent high efficiencies over 25% are mainly driven by IBC, passivated contacts (HJ, TOPCon) technologies. The IBC architecture was first suggested in 1977 [8] and efficient solar cell was reported in 1984 [9]. The HJ technology using amorphous Si (a-Si:H) layer to passivate the crystalline Si (c-Si) surface was first reported by Sanyo (now Panasonic) in 1990 [10] and following work was reported in 2000 [11].

In this paper, we demonstrate conversion efficiency of 26.6% achieved by HJ-IBC solar cell, prepared by industrially-feasible technologies. The cell characteristics of this new result are compared with those of previous record cell (26.3% HJ-IBC) to assess the improvements [7]. We discuss how far we can go in reducing the remaining losses towards the theoretical limit by using state of the art data together with our HJ-IBC cell efficiency progress since 2014.

2. HJ-IBC cell with conversion efficiency of 26.6%

2.1. Architecture

The 26.6% HJ-IBC solar cell was fabricated using n-type Czochralski crystalline Si (c-Si) 6 in. wafer with a size of 243 cm^2, a thickness of 200 μm (wafer thickness after cell fabrication), and a resistivity of ~ 7 Ω cm. The front wafer surface was textured by anisotropic etching in order to minimize the light reflection. Rear side passivation is done by P^+ HJ layer stack (i: a-Si:H layer deposition followed by p: a-Si:H layer deposition) and N^+ HJ layer stack (i: a-Si:H layer deposition followed by n-type thin film Si layer deposition) by using capacitively coupled RF plasma enhanced chemical vapor deposition (PECVD) tool. The front passivation is done by the a-Si:H layer followed by first dielectric Antireflection (AR) layer deposition using the same PECVD tool as used for rear side. Additionally, second dielectric AR layer is deposited on first dielectric layer to minimize the reflection at front surface of the HJ-IBC cell in air.

The P^+ and N^+ HJ layers stacks are patterned into interdigitated design on the rear surface. The rear interdigitated pattern is optimized to minimize the lateral transport loss and series resistance (R_S). The

* Corresponding author.
E-mail address: kunta.yoshikawa@kaneka.co.jp (K. Yoshikawa).

http://dx.doi.org/10.1016/j.solmat.2017.06.024
Received 6 April 2017; Received in revised form 13 June 2017; Accepted 16 June 2017
Available online 26 June 2017

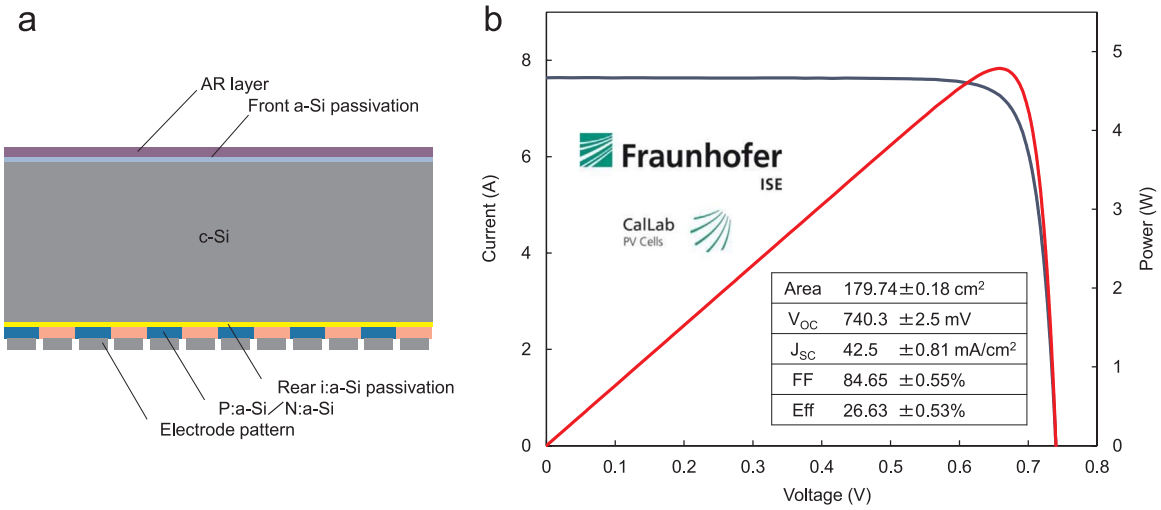

Fig. 1. (a) Cross-sectional schematic drawing of the HJ-IBC solar cell; (b) IV curve (blue line), power-voltage curve (red line) and IV parameters of the HJ-IBC solar cell. (For interpretation of the references to color in this figure legend, the reader is referred to the web version of this article.)

electrode structure is formed on both p: a-Si:H and n: a-Si:H layer to form good ohmic contact.

The designated area is designed to be square area of ~ 180 cm^2 which is centered to the wafer center. The electrodes that collect current from each finger electrodes are extended to outside of the wafer and then probed from the front side. Due to this electrode structure which lay outside of the aperture area, the measurement area is defined as designated area according to the definition given by Green [12].

2.2. IV characteristic

The schematic cross-section of the HJ-IBC solar cell and the current-voltage (IV) curve are shown in Fig. 1. The conversion efficiency of 26.6% was obtained with open circuit voltage (V_{OC}) of 0.740 V, short circuit current density (J_{SC}) of 42.5 mA/cm^2, and fill factor (FF) of 84.6%. This result was certified by Fraunhofer Institute for Solar Energy Systems (ISE) with designated area (179.7 cm^2) measurement under standard test conditions (25 °C and an illumination of AM1.5 spectrum and 100 mW/cm^2). The measured J_{SC} in IV measurement is consistent to the J_{SC} calculated from spectral response measurement also performed in Fraunhofer ISE.

Although the improvement from previous record is 0.3% absolute, considering the gap between the theoretical limit efficiency (29.4% [13]) and the previous record efficiency (26.3%), this improvement can be regarded as 10% reduction of the remaining loss.

2.3. Comparison of 26.6% and 26.3% HJ-IBC cell

In this subsection, we compare the result of this work (26.6% HJ-IBC) with the previous work (26.3% HJ-IBC). Table 1 describes the IV parameters and wafer properties of both cells respectively. The 26.6% HJ-IBC cell is fabricated using 200 μm thick c-Si wafer which is 35 μm thicker than that of 26.3% HJ-IBC cell. The 0.47% relative loss of V_{OC} and 0.59% relative gain of J_{SC} compensate each other and only leaves 0.12% gain. The main improvement of the efficiency is coming from the remarkable 1.04% relative gain of FF from 83.8% [7].

Such difference of IV parameters are also clear from the comparison of IV curves shown in Fig. 2(a). The IV curve of this work shows higher J_{SC}, lower V_{OC} and higher FF due to larger slope above 0.65 V. From the comparison of external quantum efficiency (EQE) spectra shown in Fig. 2(b), also both measured at Fraunhofer ISE, the higher EQE of 26.6% HJ-IBC in long wavelength range (900–1200 nm) indicates that the J_{SC} improvement of 0.59% is mostly coming from the wafer thickness increase or rear optical improvement. Together with the increased wafer thickness from 165 μm to 200 μm and rear side optical improvement, the J_{SC} gain of 0.23 mA/cm^2 is estimated from the EQE in 900–1200 nm range.(Fig. 3)

In wavelength range of 450–900 nm, both EQE show linear increase from ~ 0.97 to maximum with increasing wavelength. We think the origin of this EQE trends are common for 26.3% [7] and 26.6% HJ-IBC cells since the front architecture designs are similar in both cells. For 300–900 nm wavelength range, the EQE shows lower value from unity which is equivalent to 0.67 mA/cm^2. We think the major losses are parasitic absorption loss of the front side and reflection loss. It should be note that, in this wavelength range, 2–3% uncertainties of the EQE measurement are stated by Fraunhofer ISE.

In our previous work, we have shown that FF of 83.8% with pseudo FF (pFF: FF excluding series resistance) of 85.7% and R_S of 0.32 Ω cm^2 [7]. In order to specify the contribution of pFF and R_S for 26.6% HJ-IBC, pseudo IV curve from Suns-VOC measurement [14] is compared with real IV curve of 26.6% HJ-IBC cell. The Suns-V_{OC} measurement is carried out in-house using Sinton Suns-V_{OC} system under controlled temperature of 25°. The illumination intensity at cell surface is calibrated to have the same V_{OC} as certified IV result at 1 sun illumination. Due to short flash of the Suns-V_{OC} tester, the temperature increase is negligible. Due to short flash of the Suns-V_{OC} tester, we think the temperature increase is negligible.

The pFF obtained from the pseudo IV curve is 85.8%, which is very close to pFF = 85.7% from 26.3% HJ-IBC cell [7]. By fitting the pseudo IV curve to the real IV curve, the R_S of 26.6% HJ-IBC is estimated to be

Table 1
The IV parameters, wafer thickness and wafer resistivity of 26.3% HJ-IBC and 26.6% HJ-IBC.

	V_{OC} [V]	J_{SC} [mA/cm2]	FF%	η%	Cell area [cm^2]	Wafer thickness [μm]	Wafer resistivity [Ohm.cm]
26.3% HJ-IBC [7]	0.744	42.3	83.8%	26.33%	180.4	165	3
26.6% HJ-IBC	0.740	42.5	84.6%	26.63%	179.7	200	7
Relative change%	−0.47%	+ 0.59%	+ 1.04%	+1.16%	–	–	–

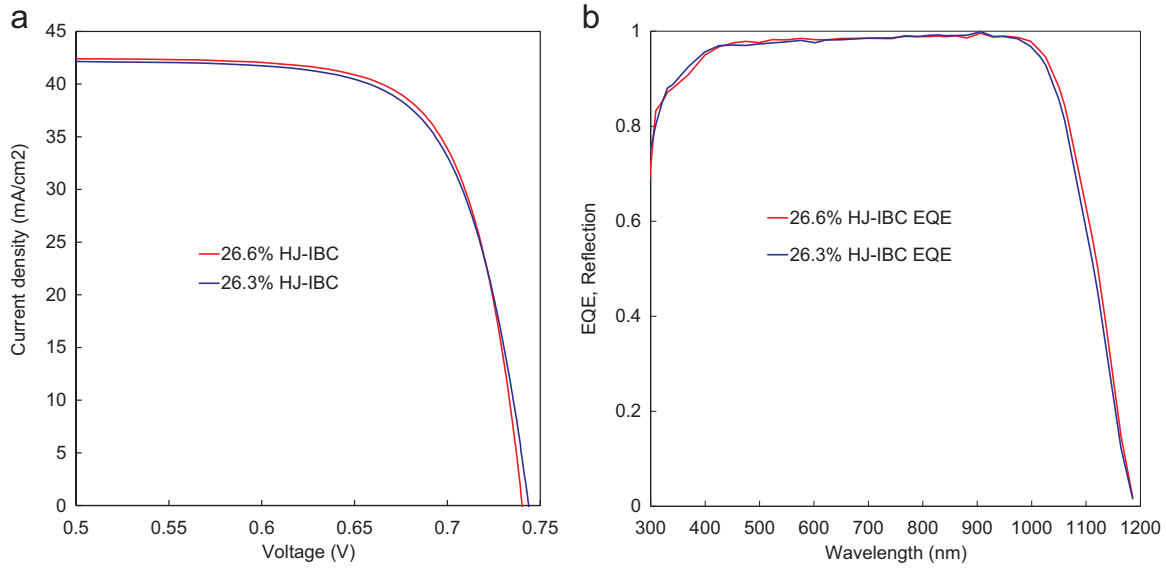

Fig. 2. (a) Comparison of IV curve; (b) Comparison of EQE spectra. The result of 26.6% HJ-IBC cell from this work and 26.3% HJ-IBC cell from our previous work [7] are shown as red and blue line respectively. (For interpretation of the references to color in this figure legend, the reader is referred to the web version of this article.)

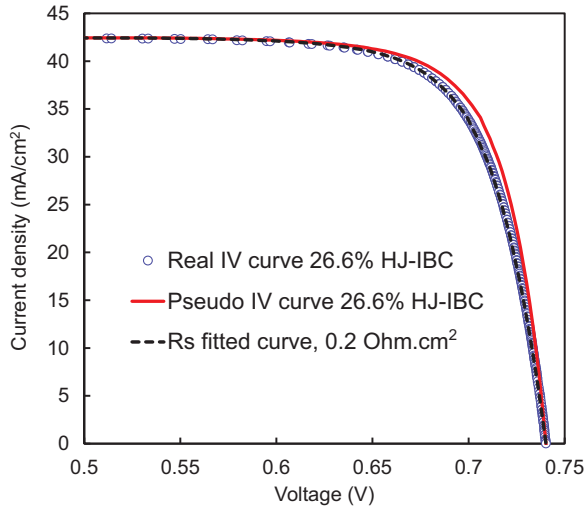

Fig. 3. Pseudo IV curve (red line) from Suns-V_{OC} and real IV curve (blue circle) of the 26.3% HJ-IBC cell. The pseudo IV curve is constructed by V_{OC}- J_{SC} (suns) plot at different intensity. The illumination intensity is monitored by a calibrated reference cell. By fitting the pseudo IV curve to the real IV curve (black dotted line), R_S of the HJ-IBC cell is estimated to be 0.2 Ω cm^2. (For interpretation of the references to color in this figure legend, the reader is referred to the web version of this article.)

Table 2
Comparison of V_{OC} and FF related parameters.

	V_{OC}, (iV_{OC}) [V]	pFF% (iFF %)	R_S [Ohm.cm^2]	FF% (calculated)
26.3% HJ-IBC [7]	0.744	85.7%	0.32	83.8%
Estimated practical limit [7]	(0.748)	(86.6%)	0.25	(85.6%)
26.6% HJ-IBC	0.740	85.8%	0.2	84.6%

~ 0.2 Ω cm^2. This is lower than R_S = 0.32 Ω cm^2 extracted from 26.3% HJ-IBC cell [7]. Thus, we can say that FF improvement from 26.3% is mostly due to nearly 30% reduction of R_S. We think the reduction of R_S is mainly coming from the reduction of interface resistance and grid resistance. The estimated R_S of 0.2 Ω cm^2 is even lower than the predicted R_S of 0.25 Ω cm^2 used for estimating the practical limit efficiency of 27.1% [7], however the change in practical limit is very small (< 0.1% absolute). These FF related parameters (V_{OC}, pFF, R_S, FF) of 26.3% HJ-IBC cell, practical limit and 26.6% HJ-IBC cell are described respectively in Table 2.

Considering the implied FF (iFF) of 86.6% from the practical limit [7], there are still room to improve the pFF of 26.6% HJ-IBC. The effective lifetime (τ_{eff}) from the Sun-V_{OC} data [14] and calculated intrinsic lifetime (τ_{intr}) [15] is shown in Fig. 4(a). The τ_{eff} shows maximum value of ~ 8 ms and decreases as excess carrier density increases. The τ_{intr} is consist of Auger and radiative lifetime and generally dominates the effective lifetime at high injection region due to strongly increasing Auger recombination with excess carriers increase. A clear discrepancy exist between τ_{eff} curve and calculated τ_{intr} curve [15] at high carrier density region above ~ 1.0 ×10^{16} cm^{-3}, where τ_{eff} curve is expected to asymptote to τ_{intr} curve in general as Auger recombination becomes dominant.

By reciprocal subtraction, shown as Eq. (1), we have estimated the extrinsic lifetime (τ_{extr}) which contains other lifetime elements such as surface recombination and the Shockley-Read-Hall (SRH) recombination due to defects in Si wafer.

$$\frac{1}{\tau_{extr}} = \frac{1}{\tau_{eff}} - \frac{1}{\tau_{intr}} \quad (1)$$

The τ_{extr} curve shows similar lifetime value and strong decay slope as those of τ_{intr} above excess carrier density of 1 ×10^{16} cm^{-3}. It should be noted that depending on the origin of this strong τ_{extr} lifetime decay at high injection, the τ_{extr} curve extracted from τ_{eff} contains other elements than just surface recombination and SRH. It is known that for lowly doped Si wafer, a-Si:H passivated surface shows strong injection level dependence [16], which may be an explanation for slight decrease of τ_{extr} observed at low injection level (1 ×10^{14} cm^{-3}) in Fig. 4(a). We think these injection dependences observed in Suns-V_{OC} are important as these may influence the achievable pFF by HJ-IBC cell.

It is known that injection dependence can be influenced by field effect of the HJ passivation [16]. For HJ-IBC solar cell, the rear design such as hole contact/electron contact ratio would change the field effect and can influence the injection dependence. However, depending on the injection dependence, the pFF could be increased by decreasing V_{OC}. Thus, especially for such strong injection dependent device, lifetime or V_{OC} at MMP is more directed to conversion efficiency excluding R_S.

The trend of low effective lifetime at high excess carrier density is expression of lower V_{OC} at high illuminations from the Suns-V_{OC}

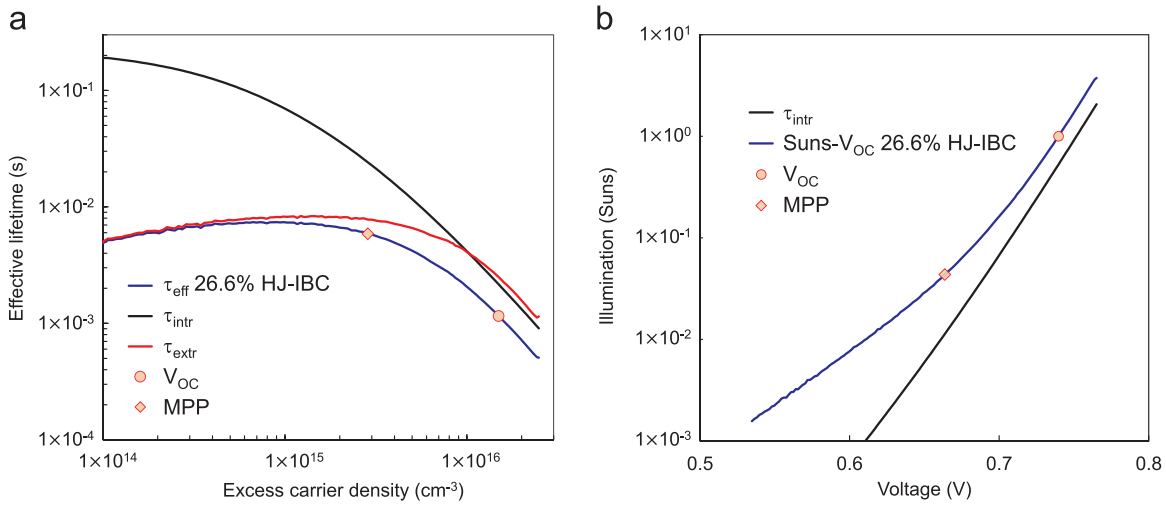

Fig. 4. (a) τ_{eff} of the 26.6% HJ-IBC cell extracted from the Suns-V_{OC} data (blue line) with V_{OC} point (red circle) and maximum power point (MPP: red diamond), calculated τ_{intr} (black line) [15] and estimated τ_{extr}. (b) Suns-V_{OC} plot of 26.6% HJ-IBC cell (blue line) and Suns-V_{OC} calculated from τ_{intr} (black line). (For interpretation of the references to color in this figure legend, the reader is referred to the web version of this article.)

measurement shown in Fig. 4(b). The HJ-IBC cell requires 2 times as higher illumination to achieve the same V_{OC} as τ_{intr} at high illumination level. This lower V_{OC} at high illumination compared to the intrinsic limit was also observed for 26.3% HJ-IBC cell. Such phenomenon in Suns-V_{OC} can be explained by higher Auger recombination than the model or voltage decrease due to partially Schottky contact [14,17], the injection dependence brought by field effect [16] or existence of barrier at c-Si/a-Si:H interface [18].

However, for 26.6% HJ-IBC cell with low R_S, influences (contact or c-Si/a-Si:H barrier) that can also induce additional R_S should be relatively lower. Therefore, we think the strong injection dependence is due to field effect coming from rear P+ HJ and N+ HJ. The field effect influences the lifetime by reducing or increasing one type of the carrier density near the recombination interface [16]. Since HJ-IBC solar cell have smaller P+HJ and N+HJ region from those of top/rear contacted HJ solar cell, and also may have different hole /electron contact ratio, influence on lifetime from the field effect has more chance to be pronounced.

3. Further efficiency improvement

3.1. Efficiency progress of HJ-IBC in c-Si

The updated progress of c-Si solar cell [1], HJ-IBC [2,19–30] and top/rear HJ [4,31] and are shown in Fig. 5 as remaining loss to the theoretical limit [13] plotted as progress time assuming progress starting date. The progresses of c-Si is picked up from Green et al. [1]. Recent result of IBC [3] and TOPCon cell results [5,6] and our previous works [7] are added together with the result of this work. The progress of the c-Si cell is divided before and after the use of passivated emitter (PE) as progress made a remarkable transition [1].

Except for top/rear HJ, by assuming the “progress starting date”, progresses are possible to fit by fractional function (R=C/T + L), where L as estimated limit, T as progress time and C as remaining value from L at T = 1 year. Most case the required progress time increases strongly as the remaining loss approaches L. It should be noted that the L is estimated limit by fitting the progress in the past and would not limit or guarantee the further progress. The top/rear HJ differs from such trend probably due to different interaction as most of the progress was done by single organization.

The progress of our HJ-IBC efficiency is shown in Fig. 6 as double logarithmic plot of remaining absolute loss towards the theoretical limit [13] respect to the development time. The development time is defined as elapsed time after we started the development of HJ-IBC in 2014.

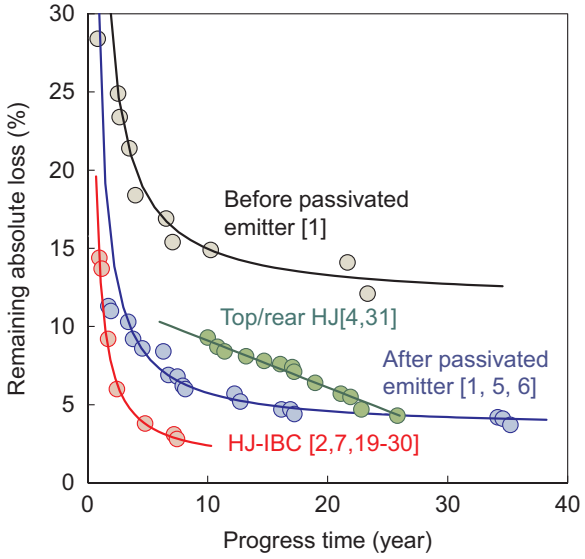

Fig. 5. The progress of c-Si solar cell without PE [1], c-Si with PE [1,3,5,6], HJ-IBC [2,7,19–30] and top/rear HJ [4,31]. Black, blue and red lines are fitted curve by fractional function for c-Si before PE, after PE and HJ-IBC progress respectively, while green line is linier fit for top/rear HJ. (For interpretation of the references to color in this figure legend, the reader is referred to the web version of this article.)

Note that the result of remaining losses higher than 6% are from in-house measurement.

Starting with efficiency below 3% with more than 26% absolute remaining loss, the efficiency improved to ~ 21% with remaining absolute loss of ~ 8.5% in ~ 2 months. Thanks to many reports of HJ-IBC cell [2,19–30] and our top/rear HJ technology reachable to efficiency of 25.1% [4], the development in initial stage was straight forward.

The subsequent progress was more gradual compared to our initial stage. The required development time increased as we reduce the remaining absolute loss.

According to the latest trend of our 3 certified results (Eff. 26.3–26.6%) shown in the Fig. 6, the achievement of practical limit efficiency (27.1%) seems promising, however, not easy.

3.2. The pFF improvement by enhanced injection dependence

After reaching 26.6%, we have focused on improving pFF which remained in similar value during the development from 26.3% to

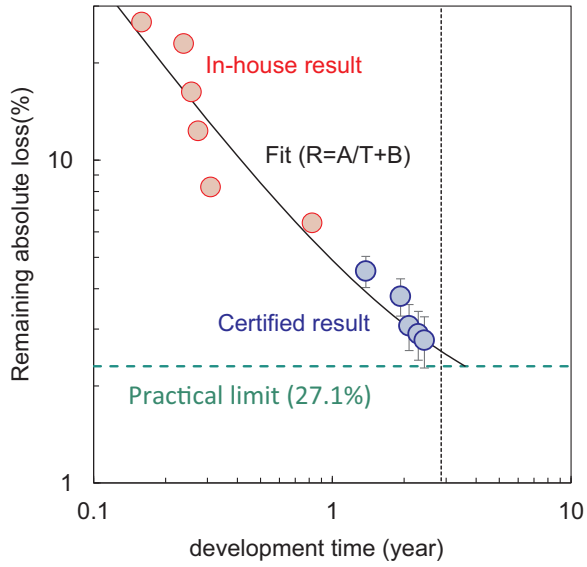

Fig. 6. The progress of our HJ-IBC efficiency from the start is shown as remaining loss to theoretical limit (29.4% [13]) respect to development time.

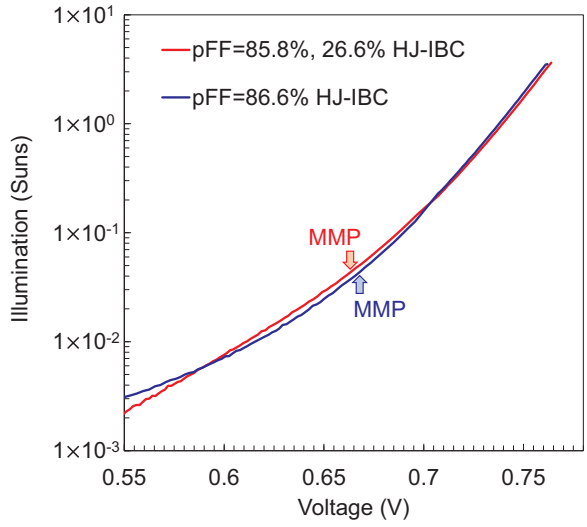

Fig. 7. Comparison of Suns-V_{OC} curve of pFF = 86.6% HJ-IBC cell (blue line) and 26.6% HJ-IBC cell (red line). The MMP of both curves are indicated by coloured arrows respectively. The same J_{SC} is used for 1 sun intensity as that of 26.6% HJ-IBC cell. (For interpretation of the references to color in this figure legend, the reader is referred to the web version of this article.)

26.6%. Recently, we have developed HJ-IBC cell with pFF of 86.6% with enhanced injection dependence, where the Suns-V_{OC} curve is compared with that of 26.6% HJ-IBC cell in Fig. 7. The 86.6% pFF curve shows 1–2 mV lower V_{OC} at 1 sun illumination while 4–5 mV higher V_{OC} at MMP (~0.044 Sun), thus the injection dependence of the Suns-V_{OC} curve is even pronounced compared to 26.6% HJ-IBC. By assuming R_S = 0.2 Ω cm^2, FF of 85.5% can be calculated, which is close to that of the practical limit [7]. However, due to lower product of J_{SC} and V_{OC}, the expected efficiency would be 26.8–26.9%, which is still far from 27.1%. Considering these injection dependences observed in HJ-IBC cell, most probably the practical limit would be realized by combination of lower V_{OC} and higher FF (pFF) compared to the estimated values described in Table 2.

We think that there are not much solutions left in our current technology to increase the FF by means of lifetime improvement or R_S reduction. Therefore, our next approach would be to improve the J_{SC}. Despite of the front electrode loss, the top/rear contacted homojunction/TOPCon cell [5,6] exhibits same J_{SC} (42.5 mA/cm^2) as 26.6% HJ-IBC with same thickness of Si wafer (~ 200 μm). We think these fact indicate that there are still possibility to obtain higher J_{SC} by HJ-IBC.

4. Conclusions

We have demonstrated efficiency of 26.6% by HJ-IBC cell with 0.3% absolute (1.16% relative) improvement from the previous record (26.3%) [7]. By comparison of IV and EQE results and Suns-V_{OC} analysis, the relative improvement of 1.16% was broken down to 0.12% gain mainly due to wafer selection and 1.04% gain coming from 30% reduction of R_S with estimated value of ~ 0.2 Ω cm^2. Similar to 26.3% HJ-IBC cell [7], the Suns-V_{OC} curve of 26.6% HJ-IBC cell showed slight bending to have lower V_{OC} at high illumination.

Despite of the extrapolation of our latest HJ-IBC progress trend, the practical limit efficiency of 27.1% is still difficult to realize. As one of the recent progress, we have shown Suns-V_{OC} result with pFF of 86.6% together with the enhanced injection dependence of the Suns-V_{OC} curve which allowed to predict the conversion efficiency of 26.8%. We think this predicted efficiency is attainable, however additional 0.3% absolute progress required to achieve the practical limit remains challenging.

Acknowledgements

This work was supported in part by the New Energy and Industrial Technology Development Organization (NEDO) under the Ministry of Economy, Trade and Industry of Japan.

References

[1] M.A. Green, The path to 25% silicon solar cell efficiency: history of silicon cell evolution, Progress. Photovolt. Res. Appl. 2009 (17) (2009) 183–189.
[2] K. Masuko, et al., Achievement of more than 25% conversion efficiency with crystalline silicon heterojunction solar cell, IEEE J. Photovolt. 4 (2014) 1433–1435.
[3] D.D. Smith, et al, Silicon solar cells with total area efficiency above 25%, Proceedings of the 42nd IEEE PVSC, 2016, pp. 3351–3355.
[4] D. Adachi, J.L. Hernandez, K. Yamamoto, Impact of carrier recombination on fill factor for large area heterojunction crystalline Si solar cell with 25.1% efficiency, Appl. Phys. Lett. 107 (2015) 233506.
[5] A. Richter, et al., Silicon solar cells with passivated rear contacts: Influence of Wafer Resistivity and Thickness, SiliconPV 2017 (2017) (Freiburg).
[6] S.W. Glunz, et al. The irresistible charm of a simple current flow pattern -25% with a solar cell featuring a full-area back contact, Paper 2BP.1.1, European Photovoltaic Solar Energy Conference, Hamburg, September, 2015.
[7] K. Yoshikawa, et al., Silicon heterojunction solar cell with interdigitated back contacts for a photoconversion efficiency over 26%, Nat. Energy 2 (2017) 17032.
[8] M.D. Lammert, R.J. Schwartz, The interdigitated back contact solar cell: a silicon solar cell for use inconcentrated sunlight, IEEE Trans. Electron Devices 24 (1977) 337.
[9] R.M. Swanson, et al., Point-contact silicon solar cells, IEEE Trans. Electron Devices 31 (5) (1984).
[10] M. Taguchi et al. Improvement of the conversion efficiency of polycrystalline silicon thin film solar cell, Proceedings of the 5th International Photovoltaic Science and Engineering Conference on Technical Digest, Kyoto, Japan, pp. 689–692.
[11] M. Taguchi, et al., HIT cells: high efficiency crystalline Si cells with Novel structure, Progress. Photovolt. 8 (2000) 492–502.
[12] M.A. Green, K. Emery, Y. Hishikawa, D. Warta, E.D. Dunlop, Solar cell efficiency tables (version 39), Prog. Photovolt. Res. Appl. 20 (2012) 12–20.
[13] A. Richter, M. Hermle, S.W. Glunz, Reassessment of the limiting efficiency for crystalline silicon solar cells, IEEE J. Photovolt. 3 (2013) 1184–1191.
[14] R.A. Sinton, A. Cuevas, A quasi-steady-state open-circuit voltage method for solar cell characterization, Proceedings of the 16th European Photovoltaic Solar Energy Conference, WIP-Renewable Energies, 2000, 1152–1155.
[15] A. Richter, S.W. Glunz, F. Werner, J. Schmidt, A. Cuevas, Improved quantitative description of Auger recombination in crystalline silicon, Phys. Rev. B 86 (2012) 165202.
[16] S. Olibet, E. Vallat-Sauvain, C. Ballif, Phys. Rev. B 76 (2007) 035326.
[17] S.W. Glunz, J. Nekarda, H. Mackel, A. Cuevas, Analyzing back contacts of silicon solar cells by Suns-Voc-measurements at high illumination densities, Proceedings of the 22nd European Photovoltaic Solar Energy Conference (WIP-Renewable Energies), 2007, 849–853.
[18] R.V.K. Chavali, et al., A generalized theory explains the anomalous Suns-Voc response of Si heterojunction solar cells, IEEE J. Photovolt. 7 (2016) 169–176.
[19] S.K. Ji, et al. The emitter having micro-crystalline surface in silicon heterojunction IBC solar cells, Proceedings of the 21st International Photovoltaic Science and Engineering Conference on Technical Digest, Fukuoka, Japan, 3A-1O-06, 2011.

[20] N. Mingirulli, et al., Efficient interdigitated back-contacted silicon heterojunction solar cells, Phys. Stat. Sol. RRL 5 (2011) 159.
[21] T. Desrues et al. Emitter optimization for interdigitated back contact (IBC) silicon heterojunction (Si-HJ) solar cells, Proceedings of the 25th European Photovoltaic Solar Energy Conference and Exhibition, Valencia, Spain, pp. 2374–2377.
[22] B. B. Shu et al. Alternative approaches for low temperature front surface passivation of interdigitated back contact silicon heterojunction solar cell, Proceedings of the 35th IEEE Photovoltaic Specialists Conference, Honolulu, Hawaii, p. 003223.
[23] S. De Iuliis et al. Interdigitated back contact amorphous/crystalline silicon solar cells. Tech. Digest, Proceedings of the 17th International Photovoltaic Science and Engineering Conference, Fukuoka, Japan, pp. 397–398.
[24] A. Hertanto et al. Back amorphous -crystalline silicon heterojunction (bach) photovoltaic device, Proceedings of the 34th IEEE Photovoltaic Specialists Conference, Philadelphia, Pennsylvania, p. 001767.
[25] S. Harrisona, et al., Back contact heterojunction solar cells patterned by laserablation, Energy Procedia 92 (2016) 730–737.
[26] T. Desrues, et al., Influence of the emitter coverage on interdigitated back contact (IBC) silicon hetero-junction (SHJ) solar cells, in Proceedings 40th IEEE Photovoltaic Spec. Conference, 2014, 857–886.
[27] S.Y. Lee, et al., Analysis of a-Si: H/TCO contact resistance for the Si heterojunction back-contact solar cell, Sol. Energy Mater. Sol. Cells 120 (2014) 412–416.
[28] A. Tomasi, et al., Backcontacted silicon heterojunction solar cells with efficiency > 21%, IEEE J. Photovolt. 4 (2014) 1046–1054.
[29] J. Nakamura, et al., Development of heterojunction back contact Si solar cells, IEEE J. Photovolt. 4 (2014) 1491–1495.
[30] B.P. Salomon, et al., Back-contacted silicon heterojunction solar cells: optical-loss analysis and mitigation, IEEE J. Photovolt. 5 (2015) 1293–1303.
[31] M. Taguchi, et al., 24.7% record efficiency HIT solar cell on thin silicon wafer, IEEE J. Photovolt. 4 (2014) 96–99.